

# Coexistence of Downlink High-Speed Railway Communication System with TDD-LTE Cellular Communication System

Bingjun Han, Yinming Liang, Liang Huo, Xin Zhang, Dacheng Yang

Wireless Theories and Technologies Lab (WT&T)  
Beijing University of Posts and Telecommunications  
Beijing, P.R. China  
hanbingjun@gmail.com

**Abstract**—With the deployment and development of high-speed railway in the world, the corresponding research on high-speed railway communication technology has made great progress. Generally, the dedicated high-speed railway communication network is believed to be required to meet the demand of high data rate with QoS guarantee on this high-speed scenario. The long term evolution (LTE), supporting the speed of 500 km/h as well as throughput of 50M to 100M bps, has a great advantage in high-speed railway communication scenario. However, little or none of the previous research involves the aspects of coexistence between the dedicated high-speed railway communication system and the adjacent cellular network systems along the railway. Thus, in this paper, we first introduce the high-speed railway communication system as well as propose a model of it, and then evaluate its coexistence performance with macro cellular communication system based on this model. Our research results show that, when these two network systems are deployed on the same frequency band, or when macro cellular system is densely deployed in urban areas, the high-speed railway communication system will be severely affected by the inter-system interference, and additional isolation will then be needed in these cases.

**Keywords**- High-speed railway communication network; TDD-LTE; interference; macro cellular communication system

## I. INTRODUCTION

With the development of the high-speed railway technology, the related research on large-throughput data transmitting technology in high-speed scenario has gone deeper to meet the growing requirement of train passengers. Generally, it means that the technology is required to have the ability to load about 1,000 to 3,000 passengers' communication traffic in a train of 300km/h speed. It is far beyond the capacity of traditional cellular and make the building of a dedicated high-speed railway communication system (HRCS) become an inevitable choice.

There have been many literatures discussing the communication issue in the high-speed railway scenario. In the structure of HRCS, [1] describes how a heterogeneous network that comprises of satellite and W-LAN systems could be implemented in a high-speed train environment to provide internet access. In [2], theory and technology for standard

WiMAX over fiber in high speed train systems is discussed. Similarly, the structure of HRCS with GSM is described in [3]. In the modeling method, [4] presented a model of analyzing the coverage efficiency of radio over fiber network for high speed railways. In [5], a simulation model channel of high speed railway is formed and the characteristics of radio wave propagations are analyzed based on the model. The large-scale propagation characteristics and interference based on the measurement is discussed in [6], while the model of link between the train and the satellite is studied in [7]. The propagation characteristics in the train cars are discussed in [8], and the assessment of LTE-R using train model is studied in [9]. The handover schemes are studied in [10] and [11], and the estimate for Doppler frequency shift and channel is proposed in [12] and [13].

However, as we know, although there have been a lot of literatures discussing HRCS related issue, there have been still no literatures that focus on the coexistence performance of co-located macro cellular communication system (MCCS) so far, which is very important on the future deployment of HRCS.

In this paper, we proposed an HRCS architecture as well as a series of system models for this architecture. Based on the models, interference performance between HRCS and the co-located macro cellular communication system is studied.

The remainder of this paper is organized as follows. In Part II, the architecture of HRCS is introduced, which includes the outer-car and intra-car part. Then, system models are proposed in Part III, including Doppler shift model, propagation model, ACIR model, downlink demodulation and link level performance model. In Part IV, we present the simulation assumption and simulation result. Lastly, in Part V, the conclusion and our future work are introduced.

## II. SYSTEM ARCHITECTURE

In this part, the background of HSCM is introduced, including the remote radio unit (RRU) based network architecture and details of vehicle-mounted repeater which is deployed in the train carriages. Similar to [1] and [2], the basic structure of HSCM we proposed is shown in Fig. 1.

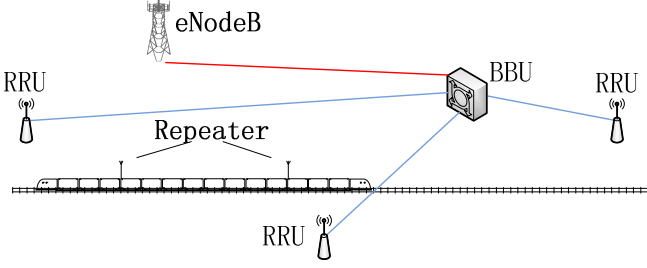


Figure 1. Structure of HRCM

In Fig. 1, RRUs are deployed along the railway track with an common figure that adjacent RRUs usually on the opposite side of the track. Several RRUs, the number of which can be configured flexibly to meet different coverage requirements, are connected with one base band unit (BBU) which can be connected with an anchor eNodeB via optical fiber [2]. Thus, less handoff is needed due to structure of the big enough virtual cell which composed of several RRUs managed by one BBU.

Compatible with the special structure of HRCS, a series of improvement is needed on the train, as shown in Fig. 2. Generally, Users inside the train carriages communicate with RRU via a vertical-mounted repeater system which acts as a transceiver between users and RRUs. This repeater system composed of leaky coaxial cables in the train which are usually used in environment like tunnels and indoor situations, the amplifier to amplify the power of the signals in the cables, the antenna which is deployed on the roof of the train to receive the RRU signals as well as a the repeater to transmit the signals in the cable. Usually, it is assumed that there are 16 carriages per high-speed train with two repeaters placed on the 4th and 12th carriage as shown in Fig. 2.

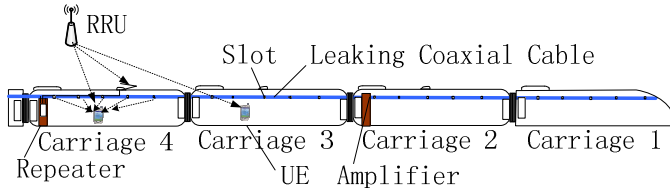


Figure 2. High-speed railway communication system based on RRUs

Each repeater serves users inside the adjacent 8 carriages. Specifically, the repeater on the 4th carriage would serve users from 1st to 8th carriage, while the repeater on 12th carriage would serve the users from 9th to 16th carriage. We configured five slots for each carriage, from which the receiving diversity can be gained, as shown in carriage 4 in Fig. 2. The propagation loss in train cars is less than that in free space [8]. One thing worth mentioning is that, different with the solution that deploy macro eNodeBs in the car, only Single Input Single Output (SISO) can be supported in HRCS because of the use of leaky cables.

### III. SYSTEM MODELS

In this part, we mainly introduce the related system models in HRCS which includes Doppler shift model in Part A, propagation loss model in Part B, adjacent channel interference radio (ACIR) modeling in Part C, downlink demodulation model in Part D as well as link level performance model in Part E.

#### A. Doppler Shift Model

The performance of data transmission is greatly affected by Doppler shift in high-speed scenario because of its fast moving character. The Doppler shift frequency  $f_D$  is defined as follows [13]

$$f_D = f_c \times v \cos \theta / c \quad (1)$$

where  $f_c$  is carrier frequency,  $v$  is velocity of the train,  $c$  is the light speed and  $\theta$  is the angle between the direction of moving speed and the direction of eNodeB or RRU which transmit the signal. In our research, the LTE system is operated at the center carrier of 2GHz and speed train can be up to 350 km/h, which means that the maximum Doppler shift frequency is about 648.15 Hz.

The bandwidth of a subcarrier with normal cycling prefix (CP) is 15 KHz, so the subcarrier spacing frequency is also 15 KHz. This ratio, which is noted as  $\alpha$ , of Doppler shift frequency and subcarrier spacing will be 4.32%. In [1], it is said that when  $\alpha$  is less than 2.5%, the Doppler shift is slight and when  $\alpha$  is greater than 5%, the Doppler shift is severe and the Doppler effects compensation is needed. [14] introduced an effective Doppler effects compensation scheme for OFDM system based on the constellation estimation to counteract inter-carrier interference (ICI). It is also easy to infer that when the carrier frequency is lower, the Doppler shift frequency will decrease, too. For example, when  $f_c = 700\text{MHz}$ , then we have  $\max(f_D) = f_c \cdot v / c = 226.9\text{Hz}$ ,  $\alpha = 226.9 / 15000 = 1.51\% < 2.5\%$  which means the Doppler shift is very slight.

#### B. Propagation Loss Models

##### 1) Outer-car propagation losses model

a) Propagation losses model between RRU and the users in the train or the repeater on top of the train

Based on our measured data on Beijing-Tianjin high speed railway in 2GHz, the propagation losses model is proposed as follows

$$L = 119.666 + 31.557 \log(d) + X_\sigma \quad (2)$$

where  $L$  denotes the propagation losses in dB, and  $d$  is the distance between the RRU and the train in kilometers.  $X_\sigma$  is log-normally distributed shadowing ( $\text{LogF}$ ) with a standard deviation  $\sigma = 10\text{dB}$ . As for users in train carriages, a penetration loss, which is relative to the grazing angle which will be talked about later, should be added to the total propagation losses. The penetration loss can be up to 25dB at carrier frequency of 2.0GHz when the grazing angle is 90

degree, in which case the direction of signal from base station is vertical with the velocity of train, and the penetration increases as the grazing angle decreases.

*b) Propagation losses model between macro cellular eNodeB and users or repeater on top of the train*

The macro cell propagation model in [15] can be used. This model is applicable for scenarios in urban and suburban areas outside the high rise core district where the buildings are of a nearly uniform height.

$$L = 40 \cdot (1 - 4 \cdot 10^{-3} \cdot D_{hb}) \cdot \log_{10}(R) - 18 \cdot \log_{10}(D_{hb}) + 21 \cdot \log_{10}(f) + 80\text{dB} \quad (4)$$

where  $R$  is the distance between the eNodeB and the repeater in kilometers;  $f$  is the carrier frequency in MHz;  $D_{hb}$  is the height of the antenna on the eNodeB in meters which is measured from the average rooftop level. After  $L$  is calculated,  $\text{LogF}$  with the standard deviation of 10dB should be added to the penetration losses for users in the carriages.

*2) Intra-car propagation losses model*

Channel Properties of the indoor part of the high-speed train is conducted in [16]. The empirical model of log-distance  $PL$  is expressed as

$$PL(d) = PL_0 + 10n \log_{10}(d) + X_\sigma \quad (5)$$

where  $PL_0$  is the intercept,  $d$  is the distance between transmitters and receivers in meters, and  $n$  is the PL exponent dependent on the specific propagation environment indicating the rate at which  $PL$  increases with distance. In free space propagation,  $n$  equals 2.  $X_\sigma$  denotes the shadow fading with a standard deviation  $\sigma$ . The propagation loss with omnidirectional antenna at transmitter is expressed as

$$PL(d) = 39.9 + 18.0 \log_{10}(d), \sigma = 2.3 \quad (6)$$

In the train carriages, leaky coaxial cable is used as shown in Fig. 2. The cable, with 5 slots in each carriage equivalent to five omni-directional antennas, can attenuate the signals transmitted on it in the rate of 60dB/25m, so an amplifier (AF) is needed to compensate the attenuation to guarantee a good receiving quality for users in every carriage. So the accumulated propagation loss is as follows.

$$L = \sum_{i=0}^5 PL_i + G_{AF} \quad (7)$$

where  $G_{AF}$  is amplifier (AF)'s gain in dB,  $PL_i$  is the propagation loss between  $i^{\text{th}}$  slot and the UE.

*C. ACIR model*

The HRCS and MCCS will interfere each other when they coexist. In calculations for this inter-system interference, the RF characteristics of transmitter and receiver are taken into account by weighting adjacent system signal with a parameter ACIR, which is defined as the ratio of the total power

transmitted from a source to the total interference power affecting a victim receiver, resulting from both transmitter and receiver imperfections [17]. The bigger ACIR means better isolation between systems, thus less power leaked to the adjacent channel. ACIR can be obtained as follows.

$$\frac{1}{ACIR} = \frac{1}{ACLR} + \frac{1}{ACS} \quad (8)$$

where ACLR reflects the spectral leakage character of transmitter, defined as the ratio of the transmitted power to the power measured in the adjacent radio frequency channel at the output of a receiver filter; ACS reflect the character of receiver, defined as the ratio of the receive filter attenuation on the assigned channel frequency to the receive filter attenuation on the adjacent channel.

*D. Downlink demodulation model*

For HRCS, its received downlink SINR can be calculated by

$$SINR_i = \frac{\sum_{l=1}^L P_{l,i} \cdot G_{l,i} \cdot PL_{l,i} + \sum_{k=1}^K P_{k,i} \cdot G_{k,i} \cdot PL_{k,i}}{\sum_{\substack{m \neq k \\ m=1}}^M P_{m,i} \cdot G_{m,i} \cdot PL_{m,i} + \sum_{n=1}^N P_{n,i} \cdot G_{n,i} \cdot PL_{n,i} + N_0} \quad (9)$$

where  $SINR_i$  is the received Signal to Interference plus Noise Ratio (SINR) for the  $i^{\text{th}}$  user (repeater);  $P_{l,i}$  is transmitted power distributed to user  $i$  from the serving RRU  $l$ ,  $G_{l,i}$  is the antenna gain of RRU  $l$  to user  $i$ ,  $PL_{l,i}$  is the path loss from RRU  $l$  to user  $i$ ;  $P_{k,i}$  is the transmitted power from the leaky coaxial cable  $k$  ( $k=1, \dots, 5$ ) to user  $i$  inside the train,  $G_{k,i}$  is the antenna gain of the leaky cable to user  $i$ ,  $PL_{k,i}$  is the path loss from the leaky cable to user,  $P_{m,i}$  is transmitted power distributed to user  $i$  from the interfering RRU  $m$ ,  $G_{m,i}$  is the antenna gain of RRU  $m$ ,  $PL_{m,i}$  is the path loss from RRU  $m$  to user  $i$ ,  $P_{n,i}$  is the interfering power from the macro base station  $n$ ,  $G_{n,i}$  is the base station's antenna gain,  $PL_{n,i}$  is the path loss from macro base station  $n$  to user  $i$  and  $N_0$  is the noise level.

*E. Link Level Performance Model*

The throughput of a modem with link adaptation can be approximated by an attenuated and truncated form of the Shannon bound, which represents the theoretical maximum throughput that can be achieved over an AWGN channel for a given SNR. The following equations approximate the throughput over a channel with a given SNR, using link adaptation. [15]

$$Thr = \begin{cases} 0 & SINR < SINR_{MIN} \\ \alpha S(SINR) & SINR_{MIN} < SINR < SINR_{MAX} \\ Thr_{MAX} & SINR > SINR_{MAX} \end{cases} \quad (10)$$

where  $S(SINR)$  is the Shannon bound  $S(SINR) = \log_2(1 + SINR)$  bps/Hz,  $\alpha$  is attenuation factor, representing implementation losses,  $SINR_{MIN}$  is the minimum SINR of the codeset in dB,  $Thr_{MAX}$  is the maximum throughput of the codeset in bps/Hz,  $SINR_{MAX}$  is SINR at which max throughput is reached  $S^{-1}(Thr_{MAX})$  in dB. The parameters proposed for the baseline E-UTRA DL is as follow [15].

TABLE I. RELATED PARAMETERS

Parameter	DL	Notes
$\alpha$ , attenuation	0.6	Represents implementation losses
$SINR_{MIN}$ , dB	-10	Based on QPSK, 1/8 rate (DL) & 1/5 rate (UL)
$Thr_{MAX}$ , bps/Hz	4.4	Based on 64QAM 4/5 (DL) & 16QAM 3/4 (UL)

#### IV. SIMULATION RESULTS

##### A. Simulation Assumptions

In our simulation, both MCCS and HRCS are TDD-LTE systems with 20MHz bandwidth and the center frequency of these systems is about 2.0GHz. The topology of HRCS and MCCS is shown in Fig.3. In this figure, the MCCS is deployed with traditional hexagonal networks with 19 cells and 57 sectors. The inter-site distance (ISD) of MCCS is configured with 500m and 1732m to simulate the urban and suburban performance. And the wrap-round algorithm is applied to eliminate the boundary effect in system level simulation. As to HRCS, the distance between two adjacent RRUs is 1500m which is shown as  $D_{RRU-RRU}$  in Fig. 3. As mentioned above, each BBU is configured with 3 RRUs and the distance between RRU and the railway is  $D_{Railway-RRU}$  in Fig. 3. In addition, 2 traditional 65 degree sectors are used in a RRU to cover the range of about 120 degree.

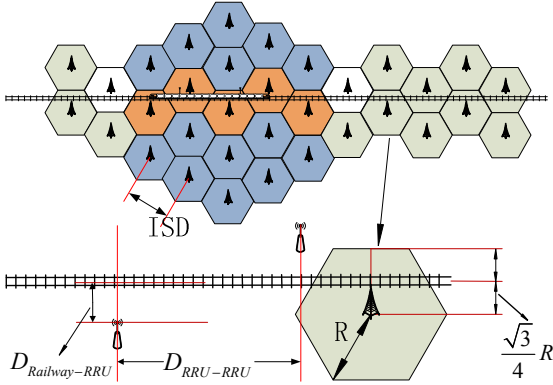


Figure 3. Topology for simulation scenario

The train in our simulation has 16 carriages which are 27 meters in length, 5 meters in height and 5 meters in width. The speed of train is 350km/h and the two repeaters, which amplify and forward signals from RRUs, are located in the 4th and 12th carriages with their antennas on top of the carriages. The antennas of repeaters can be configured as either omni-directional or directional. As mentioned above, the train is

grouped into two independent parts and each part has a repeater corresponding with users who are uniformly distributed in carriages.

The transmitting power of RRUs from HRCS and eNodeBs from MCCS is 46dBm. To meet the demand that every user in the train has a minimal receiving power of -80dBm, the power transmitted to each user from the repeater needs to be calculated. And its final value is -23.7dBm, with an amplifier in the 3rd carriage next to the carriage in which the repeater is located. There are two types of repeaters which are tested in our simulation, one is with omni-directional antennas and the other one is with directional antennas in the direction of both front and back.

In this scenario, the railway traverses the cellular cells. Moving from one cell to another will need frequent handoffs, which will cost a high load for the backbone. High penetration losses caused by Faraday cage characteristics of train are not negligible.

##### B. Simulation Results

In this section, some simulation results are listed to illustrate the coexistence performance between HRCS and MCCS. The impact of HRCS on MCCS is shown in Fig. 4 and Fig. 5. For more rational analysis, the MCCS cells are evaluated from 3 perspectives. The train traversed cells (Tr-Cells), which are shown to be orange cells in Fig. 3, the non-traversed cells (NTrCells), which are blue cells in Fig. 3, and total cells including the two categories above. The throughput loss rate of MCCS work in the same frequency band is shown in Fig. 4. From Fig. 4 we can see that MCCS is severely interfered by HRCS in the traversed cells, especially when the ISD equals 500m. However, when MCCS and HRCS work in the adjacent channel, which is shown in Fig.5, the interference is much slighter. Simulation results show that the average cell throughput loss for macro cell is below 1% in both suburban and urban scenario. In addition, the Average Throughput Loss drops as the distance between RRU and Railway increases.

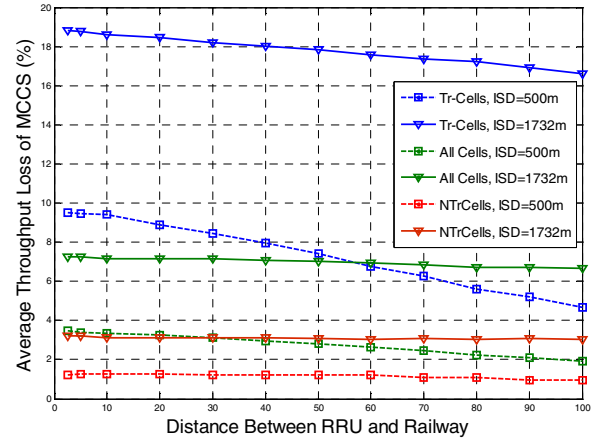


Figure 4. Throughput Loss for MCCS in Co-channel Scenario

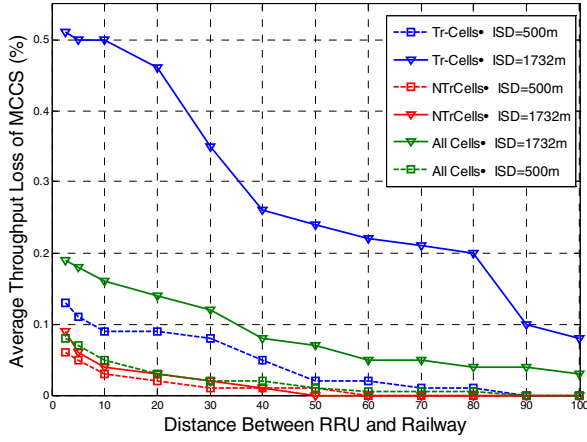


Figure 5. Throughput Loss for MCCS in Adjacent Channel Scenario

On the other hand, the simulation results for MCCS interfering HSRC are shown in Fig. 6 and Fig. 7. Our simulation results shows that throughput loss changes little as the  $D_{\text{railway-RRU}}$  changes, we can set  $D_{\text{railway-RRU}}$  to be a constant value as 50m. We calculate the capacity loss on the repeater's side and user's side respectively, and then get total throughput loss. From the two figures we can see that, contrary to the macro cellular network, the total throughput loss is greater in urban scenario. Also, the throughput loss rate is lower when repeaters with directional antennas are used. Specifically, when HSRC is co-located with MCCS on the same frequency band, as shown in Fig. 6, the throughput loss on both repeater's side and user's side are very high, especially when the ISD is 500m, the total throughput loss can be up to 90%. While the performance in adjacent channel scenario, as shown in Fig. 7, is much better. But when the ISD is 500m, the total throughput loss is up more than 14%, which is a serious interference level that cannot be ignored.

From above, we can see that it is not practical of the coexistence for HSRC and MCCS in co-channel scenario because of the high throughput loss rate. So we can consider about the coexistence on the adjacent channel scenario. However, the total throughput loss for high-speed railway network can be up to 14% in urban, while the value in suburban is below 0.5%. It means that additional isolation is needed for the urban scenario. So we simulated the relationship between ACIR and the throughput loss of HRCS in urban scenario, which is shown in Fig. 8. With the assumption that the throughput loss of HRCS is to be controlled in less than 5% and the original ACIR between HSRC and MCCS is 30dB, it is shown that additional isolation 5 dB is needed when repeaters with directional antennas are applied, while an additional isolation of at least 8 dB is needed when repeaters with omni-directional antennas are applied.

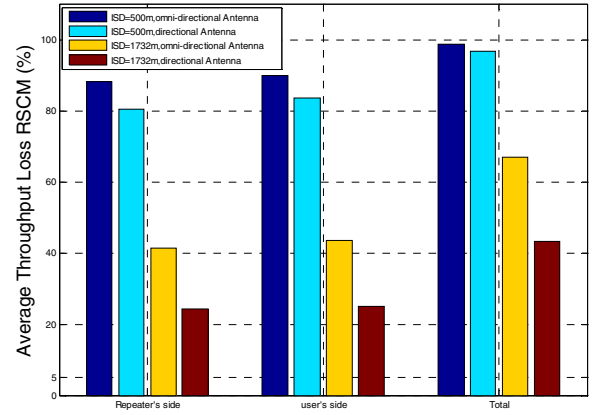


Figure 6. Throughput Loss for HRCS in Co-channel Scenario

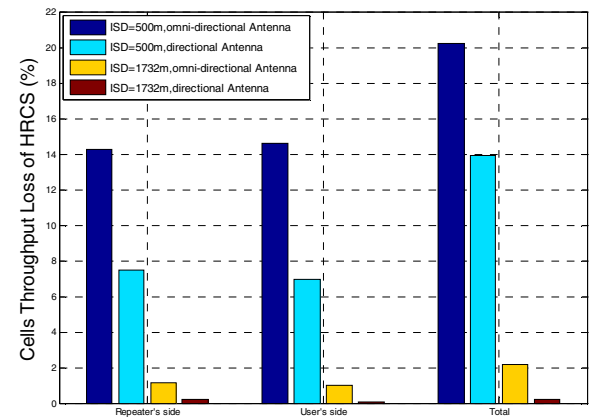


Figure 7. Throughput Loss for HRCS in Adjacent Channel Scenario

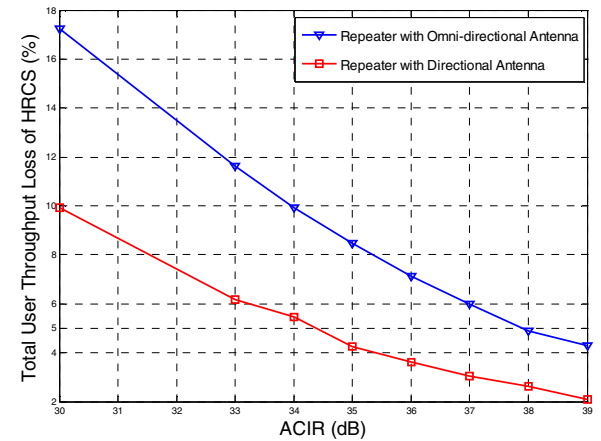


Figure 8. Total User Throughput Loss

## V. CONCLUSION AND FUTURE WORK

This paper introduces an LTE radio system solution for high-speed railway communication systems to meet the communication need of 1000 to 3000 passengers in the train of 350km/h speed. The structure of the high-speed railway communication systems (HSCS) is introduced in detail as well as the system models of HSCS. The coexistence performance of HSCS and the co-located macro cellular communication systems (MCCS) is studied based on the models mentioned above. It can be concluded that coexistence for HSCS and MCCS based on LTE in co-channel scenario is not realistic because of the high level interference from each other. The scheme of coexistence in adjacent channels is considered. The performance of this scheme for suburban scenario is excellent, while additional 5-8 dB isolation is needed for urban scenario.

For future work, some measures to reduce the interference will be studied. For example, to lower the interference from adjacent system, some measures to add isolation between HRCS and MCCS is adopted such as set guard band or take frequency scheduling algorithm. The effects of these measures need further research.

## REFERENCES

- [1] Liang, X., Ong, F.L.C., Chan, P.M.L., Sheriff, R.E., Conforto. Mobile Internet access for high-speed trains via heterogeneous networks. In: Proceedings on Personal, Indoor and Mobile Radio Communications, PIMRC 2003 14th IEEE, p.177 – 181.
- [2] C. H. Yeh, C. W. Chow, et al. Theory and Technology for Standard WiMAX over Fiber in High Speed Train Systems. *Journal of Lightwave Technology* 2010; 28(16):2327-2336.
- [3] Okada Shigeo, Kishimoto Toshihiko, et al. Leaky coaxial cable for communication in high speed railway transportation. *Radio and Electronic Engineer* 1975;45(5):224-228.
- [4] X. Cheng, Y. Li, X. Cao. The discussion on gsm coverage scheme of high-speed railway. In: Proceedings of IEEE ICCTA '09, 2009. p. 295-298.
- [5] J. Zhang, Z. Tan, X. Yu. Coverage Efficiency of Radio-over-Fiber Network for High-speed Railways. In: 2010 6th International Conference on Wireless Communications, Networking and Mobile Computing (WiCOM 2010), Sept. 2010.
- [6] Lu Qu, Yinghong Wen, Weijia Song. Research of the Characteristics of Radio Wave Propagations around the High-Speed Railway. In: 2007 4th International Symposium on EMC Proceedings, Oct. 2010. p. 405-408.
- [7] M. Berbineau, E. Masson, M. Chennaoui and J. Marais. Satellite channel modelling using a Ray-tracing Tool for train communication. In: Proceedings of 6th International Conference on ITS Telecommunications, Jun. 2006. p. 452-456.
- [8] N. Kita, T. Ito, S. Yokoyama, et al. Experimental study of propagation characteristics for wireless communications in high-speed train cars. In: 3rd European Conference on Antennas and Propagation, 2009. p. 897-901.
- [9] Ke Guan, Zhangdui Zhong and Bo Ai. Assessment of LTE-R using High Speed Railway Channel Model. In: 2011 Third International Conference on Communications and Mobile Computing, Apr. 2011. p.461-464.
- [10] Chongzhe Yang, Linghui Lu, Cheng Di, Xuming Fang. An On-vehicle Dual-antenna Handover Scheme for High-Speed Railway Distributed Antenna System. In: 2010 6th International Conference on Wireless Communications, Networking and Mobile Computing (WiCOM 2010), Sept. 2010.
- [11] K. Kastell and R. Jakoby. Implementation of fast handovers and additional authentication in GSM / UMTS for high-speed users. In: 16th IEEE Symp. on Personal Indoor and Mobile Radio Communications (PIMRC), Berlin, Germany, Sept. 2005.
- [12] J. Cho, J. Hwang, T. Hwang, H. Baik. A Novel Channel Estimation Method for OFDM in High-Speed Mobile System. In: Proceedings of IEEE International Symposium on Industrial Electronics, ISIE 2001, 2001. p. 571-574.
- [13] Xin Wang, Zhen-hui Tan, Gang Zhu, Zhang-dui Zhong. Doppler frequency shift estimation for rician channel in high-speed mobile communications. In: 2006 8th International Conference on Signal Processing, ICSP 2006.
- [14] Lee B.-S, "Doppler effects compensation scheme based on constellation estimation for OFDM system", *Electronics Letters*, vol.44, is.1, pp.38-40, Jan 2008
- [15] 3GPP TR 36.942 v9.0.1, "E-UTRA Radio Frequency (RF) systems scenarios (Release 9)", April 2010
- [16] Weihui Dong, Guangyi Liu, Li Yu, Haiyu Ding, Jianhua Zhang, "Channel Properties of indoor part for high-speed train based on wideband channel measurement" in 5th International ICST Conference on Communications and Networking in China (CHINACOM), pp.1-4, Aug 2010
- [17] 3GPP TR 25.942 V6.4.0, "Radio Frequency (RF) system scenarios," 3rd Generation Partnership Project, Technical Specification Group Radio Access Networks, Technical Report, 2005.